

Contents lists available at ScienceDirect

# Journal of Constructional Steel Research



# Local stability of laser-welded stainless steel I-sections in bending



Y. Bu \*, L. Gardner

Imperial College London, London, UK

#### ARTICLE INFO

Article history: Received 6 March 2017 Received in revised form 27 April 2018 Accepted 6 May 2018 Available online xxxx

Keywords: Bending Eurocode 3 Experiments Laser-welding Numerical modelling Stainless steel

#### ABSTRACT

Design guidance for stainless steel structures has become more comprehensive and widely available in recent years. This, coupled with a growing range of structural products and increasing emphasis being placed on sustainable and durable infrastructure, has resulted in greater use of stainless steel in construction. A recent addition to the range of structural stainless steel products is that of laser-welded sections. Owing to the high precision and low heat input of the fabrication process, the resulting sections have smaller heat affected zones, lower thermal distortions and lower residual stresses than would typically arise from traditional welding processes. There currently exists very limited experimental data on laser-welded stainless steel members and their design is not covered by current design standards. The focus of this study is therefore to investigate the cross-sectional behaviour of laser-welded stainless steel I-sections in bending. The present paper describes a series of laboratory tests performed on laser-welded stainless steel I-sections, including tensile coupon tests, initial geometric imperfection measurements and in-plane bending tests. Results of the bending tests are used to validate finite element (FE) models, which are subsequently employed for parametric investigations. The obtained experimental and FE results are used to assess the applicability of the existing design provisions of EN 1993-1-4, AISC Design Guide 27 and the continuous strength method (CSM) to laser-welded stainless steel sections. It was found that the scope of application of these existing design provisions may be safely extended to laser-welded sections.

© 2018 Elsevier Ltd. All rights reserved.

### 1. Introduction

Stainless steel is used in a wide range of engineering applications. In construction, typical applications include wall claddings, architectural components and structural elements in buildings and bridges. The broad use of stainless steel is largely attributed to the corrosion resistance, aesthetic appeal, favourable structural properties and a range of other beneficial characteristics. An innovative means of joining stainless steel is laser-welding. Laser-welding generally involves relatively low heat input, producing smaller heat affected zones, lower thermal distortions and lower residual stresses than would typically arise from traditional welding processes. The welding seams are also small, resulting in sections featuring sharp edges and corners. The use of lasers as a production tool first emerged in the late 1960s, with laser-welding maturing into an economic and practical process in the 1980s, but it is only recently that the fabrication method has gained traction in the construction industry. Hence, very limited experimental data on laser-welded stainless steel members have been reported to date. This paper presents a series of laboratory tests performed on laser-welded stainless steel I-sections in bending, together with a numerical study and the assessment of the applicability of existing design rules to these sections.

#### 2. Material properties, geometric imperfections and residual stresses

In addition to the beam tests, which are described in Section 3, a series of complementary material tensile coupon tests, stub column tests, initial geometric imperfection measurements and residual stress measurements have been carried out; a summary of these measurements is provided herein, while a more comprehensive description is given in Ref. [1].

## 2.1. Tensile coupon tests

The laser-welded I-section profiles investigated in this paper were fabricated from hot-rolled austenitic stainless steel plates (Grades 1.4307, 1.4404, 1.4571). Tensile coupon tests were conducted on the plate material and the key measured properties obtained are presented in Table 1. The adopted specimen designation system can be explained by means of an example – e.g. specimen I-102 × 68 × 5 × 5 indicates an I-section of dimensions (in mm) 102 (section height h) × 68 (section width  $b_f$ ) × 5 (web thickness  $t_w$ ) × 5 (flange thickness  $t_f$ ), with the final letter (W = web; F = flange) indicating the component from which the coupon was extracted. This notation is shown in Fig. 1. All tensile coupon tests performed herein were conducted using an Instron 8802 250 kN hydraulic testing machine, following the procedure set out in EN ISO 6892-1 [2]. The reported material properties are Young's modulus E, 0.2% proof stress  $f_y$ , 1% proof stress  $f_{1.0}$ , ultimate tensile stress  $f_{u}$ , strain at ultimate stress  $\varepsilon_u$ , strain at fracture measured over the standard

<sup>\*</sup> Corresponding author. E-mail address: y.bu13@imperial.ac.uk (Y. Bu).

**Table 1**Measured material properties from tensile coupon tests.

Specimen	t (mm)	E (N/mm <sup>2</sup> )	$f_y$ (N/mm <sup>2</sup> )	$f_{1.0}$ (N/mm <sup>2</sup> )	$f_{\rm u}$ (N/mm <sup>2</sup> )	ε <sub>u</sub> (%)	ε <sub>f</sub> (%)	Compound R-O coefficients		
								n	n' <sub>0.2,1.0</sub>	n' <sub>0.2,u</sub>
$\text{I50}\times\text{50}\times\text{4}\times\text{4}$	4.01	190,700	270	361	694	61	73	4.0	3.2	3.0
$I\text{-}102 \times 68 \times 5 \times 5$	4.99	186,800	222	331	580	50	64	3.2	3.9	3.8
$\text{I-150} \times 75 \times 7 \times \text{10-W}$	6.88	197,300	274	344	596	58	68	5.0	3.1	3.0
$\text{I-150} \times 75 \times 7 \times \text{10-F}$	9.88	197,200	267	323	560	50	66	5.0	2.7	2.7
$\text{I-160} \times \text{82} \times \text{10} \times \text{12-W}$	9.81	198,500	264	341	618	53	64	5.2	3.0	3.1
$\text{I-160} \times \text{82} \times \text{10} \times \text{12-F}$	11.69	197,500	286	342	619	52	65	7.5	2.7	2.5
$\text{I-203} \times \text{133} \times \text{6} \times \text{8-W}$	5.90	192,500	251	320	576	55	67	4.1	2.9	2.9
$\text{I-203} \times \text{133} \times \text{6} \times \text{8-F}$	7.85	192,500	281	365	597	47	64	4.2	3.4	3.3
$\text{I-220} \times 110 \times 6 \times 9\text{-W}$	6.02	193,000	275	349	670	61	71	6.0	2.9	2.8
$\text{I-220} \times 110 \times 6 \times 9\text{-F}$	8.91	197,200	292	355	671	55	65	6.2	2.5	2.6

gauge length  $\varepsilon_{\rm f}$  [2] and the strain hardening exponents for the compound Ramberg-Osgood model  $n, n'_{0.2,1.0}$  and  $n'_{0.2,u}$  [3–6]. For I-sections comprising plates of the same thickness t, a single coupon test was performed, while for sections made up of plates of different thicknesses, tensile tests on coupons extracted from both the flange (F) and the web (W) were conducted. The tested austenitic stainless steel material exhibited high ductility, with strains at fracture in excess of 50%.

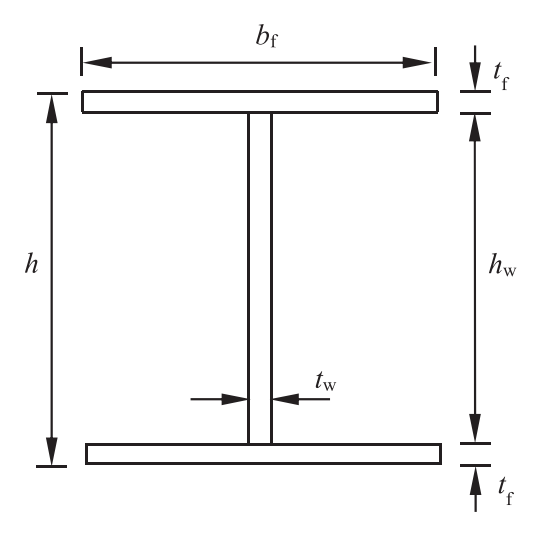


Fig. 1. Cross-section geometry and notation of test specimens.

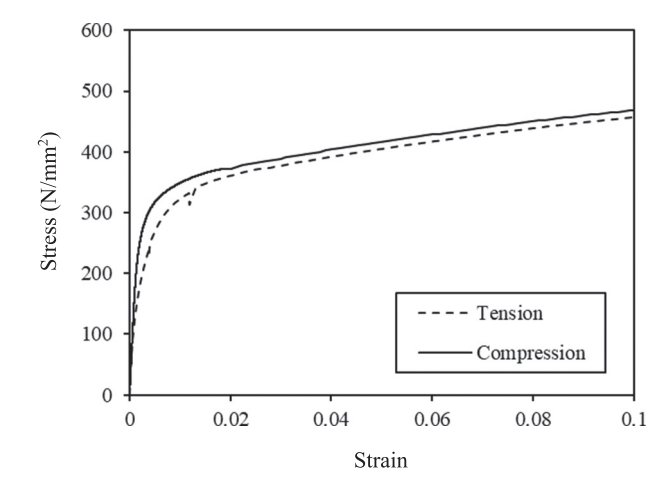


Fig. 2. Typical tensile and compressive stress-strain curves.

#### 2.2. Stub column tests

Stub column tests were conducted in accordance with the provisions of Refs. [7,8] to assess the compressive response and susceptibility to local buckling of the laser-welded I-sections, as reported in Ref. [1]. The average material properties obtained from the tests are used in this study as compressive material properties and assigned to the upper halves of the beams in the numerical simulations described in Section 4.2. The measured load-end shortening  $(N-\delta)$  responses from the stub column tests were converted into a stress-strain ( $\sigma$ - $\varepsilon$ ) curves by means of the cross-sectional area  $A_{sc}$  ( $\sigma = N/A_{sc}$ ) and length  $L_{\rm sc}$  ( $\varepsilon = \delta/L_{\rm sc}$ ). The compound Ramberg-Osgood model that utilises the 0.2% proof stress  $f_v$  and 1.0% proof stress  $f_{1.0}$  [9] was then fitted to the available stress-strain data up to the point at which local buckling initiated; beyond this point, the stress-strain curve was extrapolated in parallel with the corresponding tensile stress-strain curve up to the ultimate tensile stress. A comparison between typical tensile and corresponding compressive (extrapolated stub column) stress-strain curves (up to 10% strain) is shown in Fig. 2, while the key compressive material properties for all the tested cross-sections are summarised in Table 2 in which  $E_c$  is the compressive Young's modulus,  $f_{yc}$  is the compressive 0.2% proof strength and  $n_c$  and  $n'_{0.2,1.0,c}$  are the compound Ramberg-Osgood exponents.

## 2.3. Initial geometric imperfection measurements

Local geometric imperfections of the test specimens were measured, following the procedure reported in Ref. [10], to aid in the assessment of the structural behaviour and for later use in the numerical models. Each section size was measured to determine a representative value of local imperfection amplitude. The test piece was affixed to the flat bed of a milling machine (see Fig. 3) while a displacement transducer, attached to the head of the milling machine, was moved along a representative 600 mm length of the specimen at the cross-section locations shown

 Table 2

 Measured compressive (stub column) material properties.

Cross-section	$A_{\rm sc}$ $L_{\rm sc}$ (mm <sup>2</sup> ) (mm)		$E_{\rm c}$ (N/mm <sup>2</sup> )	f <sub>yc</sub> (N/mm <sup>2</sup> )	Compound R-O coefficients	
					$n_{c}$	n' <sub>0.2,1.0,c</sub>
$\text{I-50} \times \text{50} \times \text{4} \times \text{4}$	569.4	150.3	206,900	332	7.4	3.2
$I\text{-}102 \times 68 \times 5 \times 5$	1153.1	304.7	190,800	291	6.4	3.9
$I\text{-}140\times140\times10\times12$	4455.8	420.3	193,300	306	7.0	2.3
$I\text{-}150\times75\times7\times10$	2423.0	450.1	202,600	298	6.5	2.9
$I\text{-}152\times160\times6\times9$	3655.3	456.1	201,900	270	7.8	2.9
$I\text{-}160 \times 82 \times 10 \times 12$	3287.6	480.2	204,100	339	7.5	2.9
$I\text{-}203\times133\times6\times8$	3214.5	612.1	208,100	301	7.5	3.3
$I\text{-}220\times110\times6\times9$	3192.3	660.0	197,300	304	7.5	2.7
$I300\times150\times7\times11$	5434.3	840.0	204,100	295	8.2	2.8

# Download English Version:

# https://daneshyari.com/en/article/6750338

Download Persian Version:

https://daneshyari.com/article/6750338

<u>Daneshyari.com</u>